Nuclear Instruments and Methods in Physics Research B 541 (2023) 370–374

Contents lists available at ScienceDirect

Nuclear Inst. and Methods in Physics Research, B

journal homepage: www.elsevier.com/locate/nimb

Opportunities and limitations of in-gas-cell laser spectroscopy of the heaviest elements with RADRIS

Sebastian Raeder [a,b,*], Brankica Anđelić [a,b,c], Julian Auler [d], Michael Block [a,b,d], Pierre Chauveau [g], Premaditya Chhetri [e], Arno Claessens [e], Antoine de Roubin [e], Christoph E. Düllmann [a,b,d], Rafael Ferrer [e], Francesca Giacoppo [a,b], Manuel J. Gutiérrez [a,b], Fritz-Peter Heßberger [a], Fedor Ivandikov [e], Magdalena Kaja [i], Oliver Kaleja [a,j], Tom Kieck [a,b], Eunkang Kim [b,d], Sandro Kraemer [e], Mustapha Laatiaoui [a,b,d], Jeremy Lantis [d], Nathalie Lecesne [g], Iain D. Moore [k], Andrew Mistry [a,l,m], Danny Münzberg [a,b,d], Steven Nothhelfer [a,b,d], Andrea Raggio [k], Emmanuel Rey-Herme [h], Elisabeth Rickert [a,b,d], Jekabs Romans [e], Elisa Romero-Romero [b,d], Matou Stemmler [i], Marine Vandebrouck [h], Piet Van Duppen [e], Thomas Walther [f], Jessica Warbinek [a,d], Klaus Wendt [i]

[a] GSI Helmholtzzentrum für Schwerionenforschung GmbH, Planckstrasse 1, 64291 Darmstadt, Germany
[b] Helmholtz Institute Mainz, Staudingerweg 18, 55128 Mainz, Germany
[c] University of Groningen, Zernikelaan 25, Groningen, 9747 AA, Netherlands
[d] Department of Chemistry - TRIGA Site, Johannes Gutenberg University Mainz, Fritz-Strassmann-Weg 2, 55128 Mainz, Germany
[e] KU Leuven, Instituut voor Kern- en Stralingsfysica, Celestijnenlaan 200D, Leuven, 3001, Belgium
[f] Institute for Applied Physics, TU Darmstadt, Schlossgartenstrasse 7, 64291 Darmstadt, Germany
[g] Grand Accélérateur National d'Ions Lourds, Bd Henri Becquerel, Caen Cedex 05, BP 55027-14076, France
[h] IRFU, CEA, Université Paris-Saclay, Gif sur Yvette, 91191, France
[i] Institute for Physics, Johannes Gutenberg University Mainz, Staudingerweg 7, 55128 Mainz, Germany
[j] University of Greifswald, 17489 Greifswald, Germany
[k] University of Jyväskylä, Jyväskylä, 40014, Finland
[l] Helmholtz Forschungsakademie Hessen für FAIR (HFHF), Planckstrasse 1, 64289 Darmstadt, Germany
[m] Institute of Nuclear Physics, TU Darmstadt, Schlossgartenstrasse 9, 64291 Darmstadt, Germany

ARTICLE INFO

Keywords:
Laser spectroscopy
Gas cell
Actinides
Super heavy elements

ABSTRACT

The radiation detection resonance ionization spectroscopy (RADRIS) technique enables laser spectroscopic investigations of the heaviest elements which are produced in atom-at-a-time quantities from fusion-evaporation reactions. To achieve a high efficiency, laser spectroscopy is performed in a buffer-gas environment used to thermalize and stop the high-energy evaporation residues behind the velocity filter SHIP. The required cyclic measurement procedure in combination with the applied filament collection for neutralization as well as confinement of the stopped ions and subsequent pulse-heat desorption constrains the applicability of the technique. Here, some of these limitations and also opportunities that arise from this unique measurement setup will be evaluated.

1. Introduction

Laser spectroscopy of the heaviest elements is critical to our understanding of the atomic and nuclear characteristics of nuclides at the extreme upper end of the nuclear chart [1]. The atomic shells of such heavy elements are strongly influenced by enhanced electron correlation and relativistic effects, which alter the level scheme of the electronic orbitals and ultimately the chemical behaviour of these elements. In order to benchmark atomic theory calculations that are used to predict properties up to and beyond the heaviest known element oganesson (Og, $Z = 118$) [2], experimental data of the heaviest elements are necessary. Laser spectroscopy can be used to identify and perform a detailed characterization of electronic levels in such systems, as well as determine their ionization potentials with high precision [3]. This complements efforts focussed on studying the chemical properties

* Corresponding author at: GSI Helmholtzzentrum für Schwerionenforschung GmbH, Planckstrasse 1, 64291 Darmstadt, Germany.
E-mail address: s.raeder@gsi.de (S. Raeder).

https://doi.org/10.1016/j.nimb.2023.04.044
Received 24 February 2023; Received in revised form 1 April 2023; Accepted 22 April 2023
Available online 2 June 2023

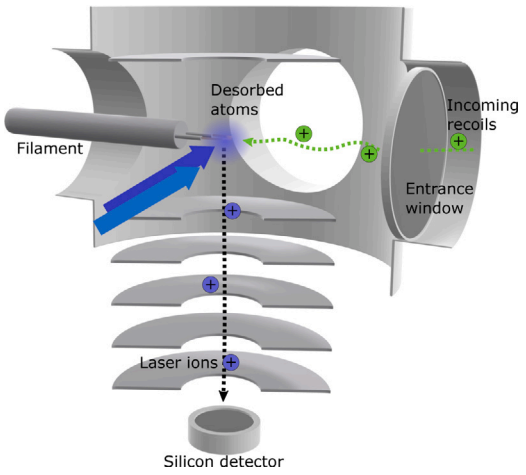

Fig. 1. Schematic drawing of the RADRIS setup. Recoils transmitted through the separator SHIP enter the gas cell passing through a thin mylar window and are collected on a catcher filament. After a half-life-dependent collection period, neutral atoms are evaporated and probed by resonance ionization spectroscopy. The resulting photo-ions are guided to the silicon detector and identified by their characteristic alpha decay energy.

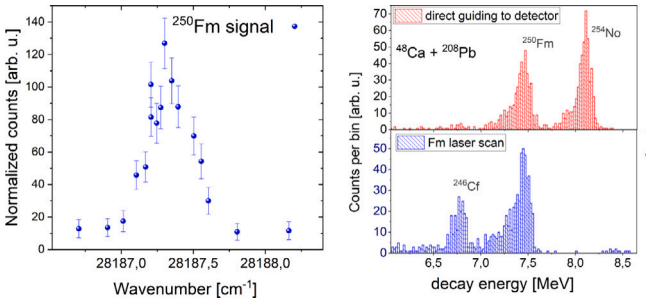

Fig. 2. Left: obtained laser resonance spectrum of ^{250}Fm for the 28 186 cm^{-1} transition which was first reported for ^{255}Fm in Ref. [19]. Right: alpha decay energy spectra obtained for direct guiding of ^{254}No to the detector (upper panel) and obtained during the laser scan of the alpha decay daughter ^{250}Fm (lower panel).

of the heaviest elements, which have been performed up to flerovium (Fl, $Z = 114$) [4]. With known atomic levels, the subtle differences in the level energies in the members of an isotopic chain, and the arising hyperfine splitting for nuclei with a non-vanishing nuclear spin can be assessed to deduce fundamental nuclear ground-state properties such as nuclear moments and spins, but also the changes of their size [5,6]. Although the atomic coupling parameters rely on atomic theory predictions [1], which are progressing towards ever more complex atomic configurations [7], the obtained nuclear parameters are not dependent on nuclear models. This is particularly important when studying the nuclear charge radii of the heaviest actinides, where strong deformation is present [8,9], leading to sub-shell effects [10].

2. Experimental methods

In this context, the radiation detection resonance ionization spectroscopy (RADRIS) technique was developed [11,12], which enabled successful laser spectroscopy of heavy actinide nuclei produced in atom-at-a-time amounts with fusion-evaporation reactions. The fusion products are produced and separated from the intense primary beam at the velocity filter SHIP at the GSI Helmholtzzentrum für Schwerionenforschung in Darmstadt [13,14]. In general, the transmitted evaporation residues feature kinetic energies of about 40 MeV, and enter the buffer gas cell through a 3.5 μm-thick aluminium-coated mylar window. Inside the experimental chamber the ions are thermalized by collisions in 95 mbar of argon gas and collected on a catcher filament by applying an attractive electrostatic potential. The ions are neutralized by touching the hafnium strip filament of 1 × 0.025 mm^2, that is typically used. Hafnium demonstrated a superior desorption behaviour during off-line tests with iso-electronic homologues compared to the previously used tantalum wires [15]. After a suitable collection time, which is determined by the half-life of the nuclide under investigation [16], the primary beam is stopped and the atoms are evaporated during a 0.3 s-long heat pulse which is monitored using a fast infrared pyrometer (LumaSense, IMPAC IS 6 Advanced). During this desorption pulse, two laser beams illuminate the region of evaporated atoms providing a two-step resonant ionization scheme.

Laser-created ions are subsequently guided towards silicon detectors enabling an unambiguous identification of the nuclides by their characteristic alpha-decay energy, which is continuously recorded. The experimental setup shown in Fig. 1 enabled laser spectroscopy of the element nobelium (No, Z=102) [17], the first optically studied transfermium element which is only available in atom-at-a-time quantities. Recent advancements of the setup for an improved efficiency and higher versatility are summarized in Ref. [18]. The application of laser spectroscopy inside the buffer gas stopping volume enables a high total efficiency, but also introduces limitations on the elements and the isotopes of a given element that are accessible to the technique. These limitations but also new opportunities will be discussed in the following sections.

3. Laser spectroscopy of decay daughter nuclei

The required cyclical collection and measurement procedure of the RADRIS technique is limited by the lifetime of the investigated nuclei due to the finite collection time as discussed in Ref. [18]. However, this mode of operation also offers a unique opportunity to use the collection cycle to breed decay daughters of the fusion-evaporation products that are collected on the filament. While the nuclei are located on the surface of the filament, many of their alpha-decay recoiling daughter nuclei are released into the buffer gas and thermalized. As they remain charged, they will be again collected on the filament surface. Losses in this breeding procedure arise from the efficiency in the applied cycle due to the lifetime of the mother and daughter nuclei. Other limiting factors are the branching ratio of the nuclear decay mode, and possible neutralization of the recoiling ions in the buffer gas. Furthermore, due to geometry, 50% of the recoils are implanted deeper into the filament and may not be released during the desorbing heating pulse which adds to the losses.

^{250}Fm ($T_{1/2}$=355 s) was one of the first isotopes investigated in this mode of operation. It was produced in the alpha decay of ^{254}No ($T_{1/2}$=52 s) with a branching ratio of $b_\alpha = 0.9$. The production of ^{254}No in the ^{208}Pb(^{48}Ca,2n)^{254}No reaction features a relatively high cross section (2 μb [20]). Also advantageous is the well understood behaviour of nobelium in a buffer-gas cell and the established atomic energy levels [17,21,22]. For laser spectroscopy of ^{250}Fm, the collection cycle was adapted such that within a 30 min collection time not only the ^{254}No ions are collected, but also the recoil decay daughters ^{250}Fm. The spectroscopic 100 Hz pulsed dye laser, pumped by an Xe:Cl excimer laser operated at 308 nm, was tuned to scan across the optical transition from the atomic ground state to an excited electronic level at 28 150 cm^{-1}, while an excimer laser operated with Xe:F at 351 nm was used as second step for non-resonant ionization. This level was first identified in reactor-bred ^{255}Fm and reported in Ref. [19]. The left graph in Fig. 2 shows the obtained optical spectrum for this transition. The right graph in Fig. 2 shows the alpha-decay energy spectrum obtained from direct collection on the silicon detector with the nobelium being present, as well as the alpha-decay energy spectrum obtained in spectroscopic measurements, where the signal of the nobelium mother vanishes. This new mode of operation will enable further measurements on nuclei

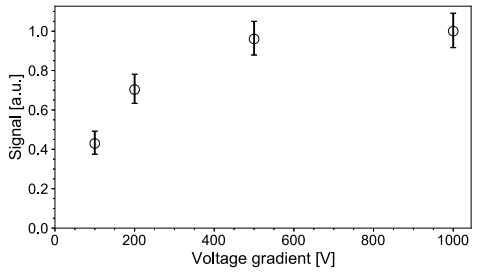

Fig. 3. Effect of the voltage gradient on the transport efficiency of the laser ions from the filament to the silicon detector on ground potential.

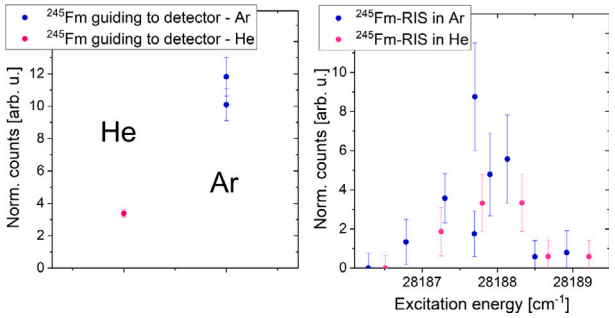

Fig. 4. Left: obtained rates for direct detector guiding for helium at 125 mbar in comparison to argon operated at 95 mbar. Here two comparable short measurements were performed for argon, while a long over-night measurement was performed with helium. Right: comparison for the obtained RIS spectra.

that are hardly available in fusion-evaporation reactions with suitable yields or beam-target combinations or which require very asymmetric fusion-evaporation reactions where the low recoil energies complicate the application of gas-cell techniques.

4. Influence of the voltage gradient and buffer gases

The filament capture technique and the guiding of the laser ions towards the detector relies on a voltage gradient created by the filament, the surrounding experimental chamber, the transport electrodes, and finally the silicon detector located on ground potential. Limitations in the efficiency of the method and the final cycle duration arise from diffusion and the ion transport time in the gas environment, which is itself limited by the ion mobility. To investigate the efficiency of the ion transport, the voltage gradient along the transport electrodes was varied by scaling the voltage setting in relation to the nominal settings. The result is shown in Fig. 3 and clearly shows that the relative efficiency is rather insensitive to the exact values of the gradient. A reduction to 25% of the nominal value still yields 50% of the maximum efficiency. Therefore, the ion transport efficiency in the typical operational conditions with 95 mbar of argon gas is not limited by diffusion losses.

A shortening of the RADRIS cycle after the filament collection and before the laser ions reach the detector would enable access to even shorter-lived nuclei. This could become possible if other inert gases such as helium or neon are used for which the ion mobility is higher and thus resulting in a faster ion transport and a shorter overall cycle period. The transport time for direct guiding to the detector was studied on-line with short-lived ^{154}Yb ($T_{1/2}$ = 409 ms) and determined to be approximately 330 ms as discussed in Ref. [18]. In addition to changes in the mobility, the achievable spectral resolution is also affected by the choice of gas, which could improve the precision for nuclear properties extracted from the hyperfine spectra. However, due to the reduced stopping power of the lighter gases and the limited stopping volume defined by the dimensions of the experimental chamber and

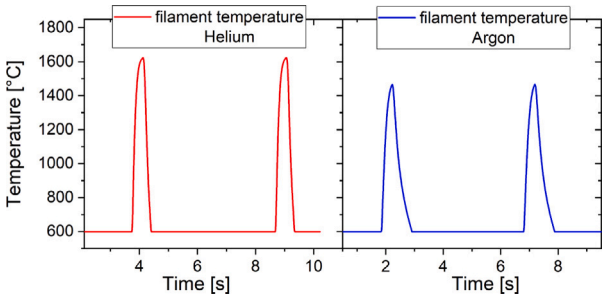

Fig. 5. Temporal profile of the hafnium filament temperature in (left) helium buffer gas at 125 mbar and (right) argon buffer gas at 95 mbar. The peak temperature is determined by the applied current and thus the heating power provided for the filament. The difference in the falling edge depends on the buffer gas due to the different heat capacities.

the extraction electrodes as shown in Fig. 1, the total efficiency might be reduced. This is problematic for laser spectroscopic investigations in this region of low recoil rates. Therefore, this effect was studied during on-line experiments comparing the performance in argon and helium gas environments.

For these tests, a 4.84 MeV/u primary ^{40}Ar beam was provided by the UNILAC at GSI, Darmstadt was used to irradiate a ^{208}PbS target wheel to produce ^{245}Fm ($T_{1/2}$ = 4.2 s) at SHIP. The first set of measurements was performed with the typical conditions for the RADRIS experiment, with argon as the buffer gas at a pressure of 95 mbar [12,18]. Initially, the ions were stopped and directly guided towards the detector as shown in the left graph of Fig. 4. In a second step, a measurement cycle with collection on a hafnium filament and laser ionization spectroscopy was performed as depicted in the right-hand graph of Fig. 4. The buffer gas was then exchanged to helium and the same two measurement cycles were performed. Here, despite a higher pressure of 125 mbar inside the buffer gas cell, the voltage gradient settings had to be reduced to avoid discharges at the electrodes. The applicable pressure inside the gas cell is limited by the thin entrance window. For collection, the central cross piece was set to a voltage of 420 V compared to the typically 1030 V used for argon [12]. The dependence of the signal intensity on the voltage gradient was not studied and therefore this voltage setting might not be optimal. The efficiency for guiding ions to the detector under these conditions was reduced by about a factor of 2.5 as shown in the left-hand part of Fig. 4. This observation is in line with the expected larger stopping distribution and the limited acceptance of the transport electrodes. When applying the collection and measurement cycle, it was also observed that the behaviour of the filament during the heating pulse was different in comparison to the typical argon environment, which is depicted in Fig. 5. Due to the increased pressure and the higher heat capacity of helium, the falling edge of the heat pulse is much steeper than in argon. When performing the laser spectroscopy on an atomic transition as shown in the right panel of Fig. 4, it becomes obvious that the loss in efficiency is less pronounced compared to the direct ion guiding, indicating that the capturing process on the filament is less sensitive to a larger stopping distribution than the direct ion guiding. Therefore, also lighter buffer gases can be considered for laser spectroscopy studies with RADRIS. The influence of the gas type on the ion transport times as well as on the laser resonance peaks will be further investigated.

5. Limitations in filament desorption

The collection and heat-pulse desorption from a catcher filament ensures on the one hand an efficient neutralization and in addition a well-confined atom-light interaction region, which is important for the required efficiencies for laser spectroscopy of the heaviest elements.

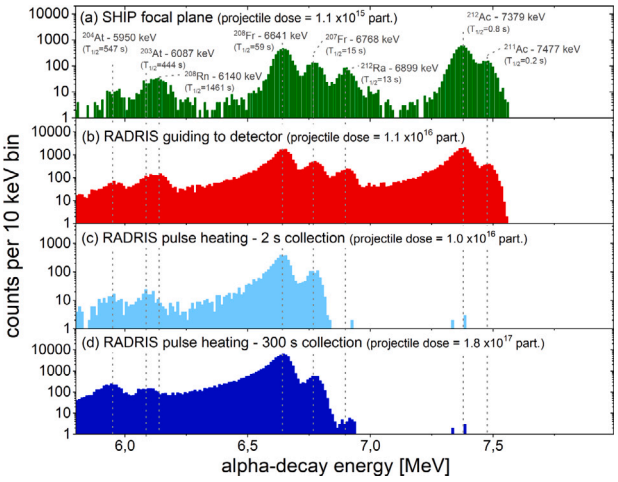

Fig. 6. From top to bottom: (a) α-decay energy spectra obtained at the SHIP focal plane detector, (b) the spectrum from RADRIS for direct guiding to the detector and two spectra obtained with two different collection times before pulse-heat desorption. The low-energy tailing for the gas-cell measurements arises from the direct collection on the silicon surface. The nuclear data are taken from Ref. [23].

On the other hand, the desorption from the filament poses an additional experimental challenge, as the required temperature, dictated by the adsorption enthalpy of the atoms of interest on the surface material, might not be reached. To test the limitation of the heat-pulse desorption, on-line produced actinium isotopes and their respective decay products were investigated with RADRIS. For actinium, well developed ionization schemes are known, and neutron deficient isotopes were investigated by in-gas-cell laser spectroscopy [24,25]. In addition, actinium features an adsorption enthalpy which is significantly higher compared to lawrencium (Lr, $Z = 100$) and especially No, and its measurement is therefore an interesting test for the evaporation of less volatile species [26]. Actinium was produced in two tests in the reaction ^{169}Tm(^{48}Ca,5n)^{212}Ac (4.55 MeV/u beam energy) and ^{175}Lu(^{40}Ar,3-4n)$^{211-212}$Ac (4.21 MeV/u beam energy). The spectra for the latter reaction obtained in different stages of the investigation are shown in Fig. 6. Here, graph 6(a) shows the alpha-decay energy spectrum obtained at the focal plane of SHIP with the directly produced $^{211-212}$Ac isotopes indicated as well as ^{212}Ra, which was produced in the p2n-evaporation channel. From a primary beam intensity of about 0.34 particleμA of $^{40}Ar^{8+}$, a detector efficiency of 55%, and a SHIP transmission of 30%, a cross section of $\sigma \approx 20$ μb for detected events can be deduced, which is similar to values reported in Ref. [27]. The pattern obtained from direct guiding to the detector, c.f. Fig. 6(b), differs only slightly, especially for ^{211}Ac and for ^{208}Rn, which is the decay daughter of ^{212}Ra. For ^{211}Ac, the short half-life of $T_{1/2} = 210$ ms already introduces losses during the process of guiding to the detector, which was investigated for ^{154}Yb in RADRIS [18] and the cryogenic gas cell at SHIPTRAP [28].^{208}Rn on the contrary is gaseous at room temperature and recoils released from the detector surface are therefore lost and only the fraction of recoils which are implanted into the detector contributes to the measured alpha-decay events. Applying a filament collection and heat-desorption cycle as shown in Fig. 6(c,d), the actinium isotopes as well as the ^{212}Ra vanish. To study the filament desorption, a short cycle with 2 s collection time, laser resonance ionization with the well-established first excitation step [24,25], and high-power non-resonant laser light at 355 nm from a Nd:YAG laser for ionization was applied. In addition, different filament materials such as Hf and carbon-coated WThO, which are discussed in more detail in Ref. [15], were studied here. Although temperatures up to 2000 °C were investigated, at which the filament material did only survive for some dozens of cycles, no signal neither resonant nor stemming from surface ionization was observed as shown in Fig. 6(c). Nevertheless, a strong signal from the daughter nuclei ^{207,208}Fr was visible from surface ionization, which could not be prevented due to the very low ionization potential of only 4.07 eV [29]. A last set of measurements, shown in Fig. 6(d), for studying the lifetimes of these isotopes, which is still under evaluation, was performed with a 300 s collection time without any laser excitation and ionization. Here, the ^{207}Fr decay with a half-life of $T_{1/2} = 15$ s is suppressed due to decay during the collection cycle. These investigations show that isotopes of elements that are volatile at room temperature such as radon cannot be collected and are thus not accessible, while high-temperature stable, refractory elements are not desorbed from the filament. Nevertheless, in conjunction with the operation mode of filament breeding as discussed earlier, refractory elements can be used to efficiently produce and study more volatile daughter nuclei, which may open up a possibility in the production of e.g. ^{256}No from the electron capture decay of the significantly less volatile ^{256}Lr.

6. Conclusion and summary

We have investigated the possibilities and limitations associated with the cyclic operation and the heat-pulse desorption used in the RADRIS technique for laser spectroscopy of exotic nuclei. The cyclic collection and measurement operation inherently allows for breeding of daughter nuclei and thus enables access to nuclei which are difficult to produce in a direct scheme. The lifetime limitations arising from the measurement cycle were investigated in Ref. [18]. Our first approach to overcome this limit was the usage of He as buffer gas. The results are promising, and encourage further investigations in this direction. The pulse-heating from the catcher filament adds an additional experimental challenge and hampers the measurement of elements where high desorption temperatures are required. Nevertheless, the element selectivity of the desorption process can also assist in the identification of recoils, as the total efficiency of the entire setup is decreased for incomplete desorption of elements with a high adsorption enthalpy. The possibility of studying decay daughters opens new possibilities, also with respect to the ongoing development of the JetRIS setup [30] which combines the high resolution of laser spectroscopy in a gas jet [31] with the filament neutralization from RADRIS. Here, daughter nuclei of refractory elements can also be studied despite the continuous operational mode of this in-gas-jet technique.

Declaration of competing interest

The authors declare that they have no known competing financial interests or personal relationships that could have appeared to influence the work reported in this paper.

Acknowledgements

This experiment has been carried out as part of FAIR-Phase-0 at the beam line Y7/SHIP at the GSI Helmholtzzentrum für Schwerionenforschung, Darmstadt, Germany. This work has been supported by the Bundesministerium für Bildung und Forschung (BMBF, Germany) under Project No. 05P18UMCIA. This project has received funding from the European Union's Horizon 2020 research and innovation programme under grant agreement No 861198–LISA–H2020-MSCA-ITN-2019. RADRIS has received funding from IN2P3-DSM/CEA and GSI under the French-German collaboration agreement number PN1064. E.K., E.R.-R. and M.L. acknowledge funding from the European Research Council (ERC) under the European Union's Horizon 2020 Research and Innovation Programme (Grant Agreement No. 819957). A.C., P.C, A.d.R., R.F., F.I., S.K., J.R. and P.V.D. acknowledge funding from the Research Foundation – Flanders (FWO) and from the EOS (nr. 30468642) project of the FWO and F.R.S.-FNRS under the Excellence of Science (EOS) programm. T.W. acknowledges funding from the Bundesministerium für Bildung und Forschung (BMBF, Germany) under grant number 05P21RDFN1. Part of the results presented in this work are also part of the PhD thesis of J.W.

References

[1] M. Block, M. Laatiaoui, S. Raeder, Prog. Part. Nucl. Phys. 116 (2021) 103834, http://dx.doi.org/10.1016/j.ppnp.2020.103834.

[2] O.R. Smits, P. Indelicato, W. Nazarewicz, M. Piibeleht, P. Schwerdtfege, Pushing the limits of the periodic table–A review on atomic relativistic electronic structure theory and calculations for the superheavy elements, 2023, arXiv preprint arXiv:2301.02553.

[3] K. Wendt, T. Gottwald, C. Mattolat, S. Raeder, Hyperfine Interact. 227 (1–3) (2014) 55, URL http://dx.doi.org/10.1007/s10751-014-1041-8.

[4] A. Yakushev, L. Lens, C.E. Düllmann, J. Khuyagbaatar, E. Jäger, J. Krier, J. Runke, H.M. Albers, M. Asai, M. Block, J. Despotopulos, A.D. Nitto, K. Eberhardt, U. Forsberg, P. Golubev, M. Götz, S. Götz, H. Haba, L. Harkness-Brennan, R.-D. Herzberg, F.P. Heßberger, D. Hinde, A. Hübner, D. Judson, B. Kindler, Y. Komori, J. Konki, J. Kratz, N. Kurz, M. Laatiaoui, S. Lahiri, B. Lommel, M. Maiti, A.K. Mistry, C. Mokry, K.J. Moody, Y. Nagame, J.P. Omtvedt, P. Papadakis, V. Pershina, D. Rudolph, L. Samiento, T. Sato, M. Schädel, P. Scharrer, B. Schausten, D.A. Shaughnessy, J. Steiner, P. Thörle-Pospiech, A. Toyoshima, N. Trautmann, K. Tsukada, J. Uusitalo, K.-O. Voss, A. Ward, M. Wegrzecki, N. Wiehl, E. Williams, V. Yakusheva, Front. Chem. 10 (2022) http://dx.doi.org/10.3389/fchem.2022.976635.

[5] P. Campbell, I. Moore, M. Pearson, Prog. Part. Nucl. Phys. 86 (2016) 127–180, http://dx.doi.org/10.1016/j.ppnp.2015.09.003.

[6] X. Yang, S. Wang, S. Wilkins, R.G. Ruiz, Prog. Part. Nucl. Phys. 129 (2023) 104005, http://dx.doi.org/10.1016/j.ppnp.2022.104005.

[7] S.O. Allehabi, V.A. Dzuba, V.V. Flambaum, Phys. Rev. A 107 (2023) 032805, http://dx.doi.org/10.1103/PhysRevA.107.032805.

[8] S. Cwiok, P.-H. Heenen, W. Nazarewicz, Nature 433 (7027) (2005) 705–709, http://dx.doi.org/10.1038/nature03336.

[9] P.-H. Heenen, J. Skalski, A. Staszczak, D. Vretenar, Nuclear Phys. A 944 (2015) 415–441, http://dx.doi.org/10.1016/j.nuclphysa.2015.07.016.

[10] E.M. Ramirez, D. Ackermann, K. Blaum, M. Block, C. Droese, C.E. Düllmann, M. Dworschak, M. Eibach, S. Eliseev, E. Haettner, et al., Science 337 (6099) (2012) 1207–1210, http://dx.doi.org/10.1126/science.1225636.

[11] H. Backe, W. Lauth, M. Block, M. Laatiaoui, Nuclear Phys. A 944 (2015) 492–517, http://dx.doi.org/10.1016/j.nuclphysa.2015.07.002.

[12] F. Lautenschläger, P. Chhetri, D. Ackermann, H. Backe, M. Block, B. Cheal, A. Clark, C. Droese, R. Ferrer, F. Giacoppo, S. Götz, F. Heßberger, O. Kaleja, J. Khuyagbaatar, P. Kunz, A. Mistry, M. Laatiaoui, W. Lauth, S. Raeder, T. Walther, C. Wraith, Nucl. Instrum. Methods Phys. Res. B 383 (2016) 115–122, http://dx.doi.org/10.1016/j.nimb.2016.06.001.

[13] G. Münzenberg, W. Faust, S. Hofmann, P. Armbruster, K. Güttner, H. Ewald, Nucl. Instrum. Methods 161 (1) (1979) 65–82, http://dx.doi.org/10.1016/0029-554X(79)90362-8.

[14] M. Block, F. Giacoppo, F.-P. Heßberger, S. Raeder, La Rivista Del Nuovo Cimento 45 (4) (2022) 279–323, http://dx.doi.org/10.1007/s40766-022-00030-5.

[15] T. Murböck, S. Raeder, P. Chhetri, K. Diaz, M. Laatiaoui, F. Giacoppo, M. Block, Hyperfine Interact. 241 (1) (2020) http://dx.doi.org/10.1007/s10751-019-1689-1.

[16] M. Laatiaoui, H. Backe, M. Block, P. Chhetri, F. Lautenschläger, W. Lauth, T. Walther, Hyperfine Interact. 227 (2014) 69–75, http://dx.doi.org/10.1007/s10751-013-0971-x.

[17] M. Laatiaoui, W. Lauth, H. Backe, M. Block, D. Ackermann, B. Cheal, P. Chhetri, C.E. Düllmann, P. Van Duppen, J. Even, et al., Nature 538 (7626) (2016) 495–498, http://dx.doi.org/10.1038/nature19345.

[18] J. Warbinek, B. Anđelić, M. Block, P. Chhetri, A. Claessens, R. Ferrer, F. Giacoppo, O. Kaleja, T. Kieck, E. Kim, M. Laatiaoui, J. Lantis, A. Mistry, D. Münzberg, S. Nothhelfer, S. Raeder, E. Rey-Herme, E. Rickert, J. Romans, E. Romero-Romero, M. Vandebrouck, P.V. Duppen, T. Walther, Atoms 10 (2) (2022) 41, http://dx.doi.org/10.3390/atoms10020041.

[19] H. Backe, A. Dretzke, R.G. Haire, P. Kunz, W. Lauth, M. Sewtz, N. Trautmann, et al., Hyperfine Interact. 162 (1–4) (2005) 3–14, http://dx.doi.org/10.1007/s10751-005-9209-x.

[20] Y.T. Oganessian, V. Utyonkov, Y.V. Lobanov, F.S. Abdullin, A. Polyakov, I. Shirokovsky, Y.S. Tsyganov, A. Mezentsev, S. Iliev, V. Subbotin, et al., Phys. Rev. C 64 (5) (2001) 054606, http://dx.doi.org/10.1103/PhysRevC.74.044602.

[21] P. Chhetri, D. Ackermann, H. Backe, M. Block, B. Cheal, C. Droese, C.E. Düllmann, J. Even, R. Ferrer, F. Giacoppo, S. Götz, F. Heßberger, M. Huyse, O. Kaleja, J. Khuyagbaatar, P. Kunz, M. Laatiaoui, F. Lautenschläger, W. Lauth, N. Lecesne, L. Lens, E.M. Ramirez, A. Mistry, S. Raeder, P.V. Duppen, T. Walther, A. Yakushev, Z. Zhang, Phys. Rev. Lett. 120 (26) (2018) 263003, http://dx.doi.org/10.1103/physrevlett.120.263003.

[22] S. Raeder, D. Ackermann, H. Backe, R. Beerwerth, J. Berengut, M. Block, A. Borschevsky, B. Cheal, P. Chhetri, C.E. Düllmann, V. Dzuba, E. Eliav, J. Even, R. Ferrer, V. Flambaum, S. Fritzsche, F. Giacoppo, S. Götz, F.H. berger, M. Huyse, U. Kaldor, O. Kaleja, J. Khuyagbaatar, P. Kunz, M. Laatiaoui, F. Lautenschläger, W. Lauth, A. Mistry, E.M. Ramirez, W. Nazarewicz, S. Porsev, M. Safronova, U. Safronova, B. Schuetrumpf, P.V. Duppen, T. Walther, C. Wraith, A. Yakushev, Phys. Rev. Lett. 120 (23) (2018) http://dx.doi.org/10.1103/PhysRevLett.120.232503.

[23] M. Bhat, Nucl. Data Sci. Technol. (2022) 817, Data extracted using the NNDC On-Line Data Service from the ENSDF database, file revised as of February 2023.

[24] C. Granados, P. Creemers, R. Ferrer, L.P. Gaffney, W. Gins, R. de Groote, M. Huyse, Y. Kudryavtsev, Y. Martínez, S. Raeder, S. Sels, C.V. Beveren, P.V. den Bergh, P.V. Duppen, K. Wrzosek-Lipska, A. Zadvornaya, A.E. Barzakh, B. Bastin, P. Delahaye, L. Hijazi, N. Lecesne, F. Luton, J. Piot, H. Savajols, J.-C. Thomas, E. Traykov, R. Beerwerth, S. Fritzsche, M. Block, X. Fléchard, S. Franchoo, L. Ghys, H. Grawe, R. Heinke, T. Kron, P. Naubereit, K. Wendt, M. Laatiaoui, I. Moore, V. Sonnenschein, M. Loiselet, E. Mogilevskiy, S. Rothe, Phys. Rev. C 96 (5) (2017) 054331, http://dx.doi.org/10.1103/physrevc.96.054331.

[25] R. Ferrer, A. Barzakh, B. Bastin, R. Beerwerth, M. Block, P. Creemers, H. Grawe, R. de Groote, P. Delahaye, X. Fléchard, S. Franchoo, S. Fritzsche, L.P. Gaffney, L. Ghys, W. Gins, C. Granados, R. Heinke, L. Hijazi, M. Huyse, T. Kron, Y. Kudryavtsev, M. Laatiaoui, N. Lecesne, M. Loiselet, F. Lutton, I.D. Moore, Y. Martínez, E. Mogilevskiy, P. Naubereit, J. Piot, S. Raeder, S. Rothe, H. Savajols, S. Sels, V. Sonnenschein, J.-C. Thomas, E. Traykov, C.V. Beveren, P.V. den Bergh, P.V. Duppen, K. Wendt, A. Zadvornaya, Nature Commun. 8 (1) (2017) http://dx.doi.org/10.1038/ncomms14520.

[26] B. Eichler, C. Frink, N. Trautmann, G. Herrmann, Fresenius Z. Anal. Chem. 335 (7) (1989) 656–662, http://dx.doi.org/10.1007/bf01204066.

[27] D. Vermeulen, H.G. Clerc, C.C. Sahm, K.H. Schmidt, J.G. Keller, G. Münzenberg, W. Reisdorf, Z. Phys. A 318 (2) (1984) 157–169, http://dx.doi.org/10.1007/bf01413464.

[28] O. Kaleja, B. Anđelić, K. Blaum, M. Block, P. Chhetri, C. Droese, C. Düllmann, M. Eibach, S. Eliseev, J. Even, S. Götz, F. Giacoppo, N. Kalantar-Nayestanaki, M. Laatiaoui, E.M. Ramirez, A. Mistry, T. Murböck, S. Raeder, L. Schweikhard, P. Thirolf, Nucl. Instrum. Methods Phys. Res. B 463 (2020) 280–285, http://dx.doi.org/10.1016/j.nimb.2019.05.009.

[29] E. Arnold, W. Borchers, H.T. Duong, P. Juncar, J. Lerme, P. Lievens, W. Neu, R. Neugart, M. Pellarin, J. Pinard, J.L. Vialle, K. Wendt, ISOLDE, J. Phys. B: At. Mol. Opt. Phys. 23 (20) (1990) 3511–3520, http://dx.doi.org/10.1088/0953-4075/23/20/014.

[30] S. Raeder, M. Block, P. Chhetri, R. Ferrer, S. Kraemer, T. Kron, M. Laatiaoui, S. Nothhelfer, F. Schneider, P.V. Duppen, M. Verlinde, E. Verstraelen, T. Walther, A. Zadvornaya, Nucl. Instrum. Methods Phys. Res., Sect. B 463 (2020) 272–276, http://dx.doi.org/10.1016/j.nimb.2019.05.016.

[31] Y. Kudryavtsev, R. Ferrer, M. Huyse, P. Van den Bergh, P. Van Duppen, Nucl. Instrum. Methods Phys. Res. B 297 (2013) 7–22, http://dx.doi.org/10.1016/j.nimb.2012.12.008.